A MOST EFFICIENT OXYGEN REDUCTION ELECTRODE – IS THIS REALIZABLE?

to be submitted by

CH. VENKATESWARA RAO

for the award of the degree

of

DOCTOR OF PHILOSOPHY

DEPARTMENT OF CHEMISTRY

INDIAN INSTITUTE OF TECHNOLOGY, MADRAS

CHENNAI – 600 036, INDIA

JANUARY 2008

1. INTRODUCTION

The electrochemical reduction of molecular oxygen is important especially for devices such as metal-air batteries, fuel cells and air cathodes in many industrial electrocatalytic processes. Oxygen reduction reaction (ORR) has been studied over the years because of its fundamental complexity, sensitivity to the electrode surface and sluggish kinetics. The sluggish kinetics of ORR under the conditions employed in electrochemical devices is due to the low partial pressure of oxygen in air, slow flow rate of oxygen (i.e., less residence time for oxygen molecules on active sites) under ambient conditions. The main disadvantage in this important electrode reaction is the value of exchange current density (j_o) in the region of 10^{-10} A cm^{-2} in acidic medium and 10^{-8} A cm^{-2} at 298 K in alkaline solution, which is lower than the j_o value of anodic reaction in the electrochemical devices. Hence the oxygen reduction reaction usually contributes considerably to the overpotential (from the equation $\eta = RT/nF \ln(j/j_o)$) and therefore results in a low efficiency in the functioning of electrochemical devices using air as oxidant (Ralph and Hogarth, 2002). Understanding and exploitation of electrocatalysis for this reaction is needed more than any other reactions in electrochemical devices.

2. OBJECTIVES AND SCOPE OF THE WORK

The essential criteria for a better oxygen reduction electrode materials are: high electronic conductivity, chemical and structural stability under the conditions namely; operating temperature, wide range of oxygen partial pressure and concentration of electrolyte, ability to decompose the intermediate species formed during the reduction process, chemical and thermomechanical compatibility to electrolyte and interconnector materials, tolerant to contaminants e.g., halide ions, methanol, NO_x, CO_x, SO_x and low cost.

Though various compositions and configurations of the electrodes have been proposed, the search for an efficient electrode has always been continuing. Even though one tends to believe that the basic principle of oxygen reduction reaction is known, the formulation of a compositional electrode satisfying the basic requirements of the components of the overall reaction has not yet been successful. This could be due to various factors inherent in extrapolation as well as the gap existing between theoretical formulation and experimental realization. Secondly, the search for an electrode especially for oxygen reduction reaction

has been based on some electrochemical parameters like the mass activity and on-set potential for which no theoretical framework has been formulated so that one can a priori predict them. If this were to be possible then formulation and design of an efficient oxygen reduction electrode might have been possible. In the absence of such a theoretical framework, one has to resort to data collection, reduction deduction methodology technique which is still empirical.

Conventional carbon supported platinum based materials are the most active, efficient, applicable and successful catalysts for oxygen reduction at the current technology stage (Gasteiger *et al*., 2005). But the formation of –OH species on the Pt electrode surface at +0.8 V vs. NHE hinder the oxygen reduction (Mukerjee *et al*., 1995). In order to compensate the loss of activity, one requires higher amounts of catalyst which dramatically increases the cost. Moreover, Pt is expensive and less abundant in nature. For the cost reduction of catalyst, two approaches are currently active: (1) reduction of Pt loading (Kinoshita, 1990; Mukerjee *et al*., 1995; Gasteiger *et al*., 2005) and (2) exploration of non-Pt based catalysts (Schulenberg *et al*., 2003; Lefe´vre *et al*., 2005; Ferna´ndez *et al*., 2005; Raghuveer *et al*., 2005; Colmenares *et al*., 2007; Tributsch, 2007).

The main objective of the present work is to develop both Pt and non-Pt based oxygen reduction electrodes for electrochemical device applications. Conventional metals and metal alloys, chalcogenide and macro-cycle based systems have been examined for the oxygen reduction reaction in this study. The thesis work focused on the following aspects.

- To synthesize carbon supported Pt nanoparticles of different sizes by polyol reduction method and study the effect of particle size on oxygen reduction.
- To synthesize carbon supported Pt alloy (Pt-Cr, Pt-Co and Pt-Fe) nanoparticles by polyol reduction method and study the role of the alloying element on the enhanced oxygen reduction activity.
- To synthesize carbon supported Pd and Pd alloys (Pd-Co-M; M = Mo and Au) by reverse microemulsion method and examine the oxygen reduction activity.
- To synthesize carbon supported Ru_xSe_y (x = 1 and y = 0, 0.2, 0.4, 0.6, 0.8 and 1.0) electrodes by reverse microemulsion method and study the optimum composition for maximum oxygen reduction activity.

- To study the facile reduction of oxygen on MN$_4$ (M = Fe and Co) clusters using Density Functional Theory (DFT).
- To synthesize MN$_4$C$_x$ (M = Fe and Co) clusters in nanosize range by pyrolyzing macrocyclic complexes and study the oxygen reduction activity.

3. SUMMARY OF THE RESEARCH WORK

3.1. Size effect of Pt nanoparticles on oxygen reduction

Monodispersed Pt nanoparticles of different sizes (2.0, 2.5, 3.5, 4.0, 5.0 and 6.0 nm) were synthesized by reduction of platinum(II)acetylacetonate with 1,2-hexadecanediol in the presence of long chain carboxylic acid and long chain alkyl amine as protecting agents. The purified Pt nanoparticles were loaded onto carbon black (CDX975, received from Columbian Chemicals Company, USA) under ultrasonic agitation to achieve 20wt.% Pt/CDX975. The prepared materials were characterized by X-ray diffraction (XRD), transmission electron microscopy (TEM) and Energy dispersive X-ray analysis (EDX) techniques. Face-centered cubic (fcc) structure of Pt was evident from the XRD. TEM images of the as-synthesized catalysts showed uniform size and shaped Pt nanoparticles on the carbon support. EDX confirms the presence of Pt and C in the catalysts. Oxygen reduction measurements were performed at room temperature by cyclic voltammetry using a potentiostat (BAS 100 electrochemical analyzer) connected to a three electrode cell assembled with glassy carbon (GC) disk as the working electrode, Ag/AgCl, 3.5 M KCl (+0.205 V vs NHE) as the reference and Pt foil as the counter electrodes, respectively. Oxygen saturated 0.5 M H$_2$SO$_4$ was the electrolyte. The electrode was fabricated as follows: 5 mg of Pt/C catalyst was dispersed in 5 ml of isopropanol by ultrasonication for 20 min. An aliquot of 20 μl catalyst suspension was pipetted onto the carbon substrate, leading to a Pt loading of 56 μg$_{pt}$ cm^{-2}. After evaporation of the water in an argon stream, 10 μl of a diluted Nafion® solution were pipetted on the electrode surface in order to attach the catalyst particles onto the GC disk. After preparation, the electrode was immersed in deaerated 0.5 M H$_2$SO$_4$. Then the linear sweep voltammogram (LSV) was recorded at a scan rate of 5 mV s^{-1} between +0.2 V and +1.2 V. For the oxygen reduction experiments, the electrolyte was saturated with pure oxygen and recorded the linear sweep voltammogram (LSV) between +0.2 and +1.2 V at a scan rate of 5 mV s^{-1}. The corresponding LSVs are shown in Fig. 1.
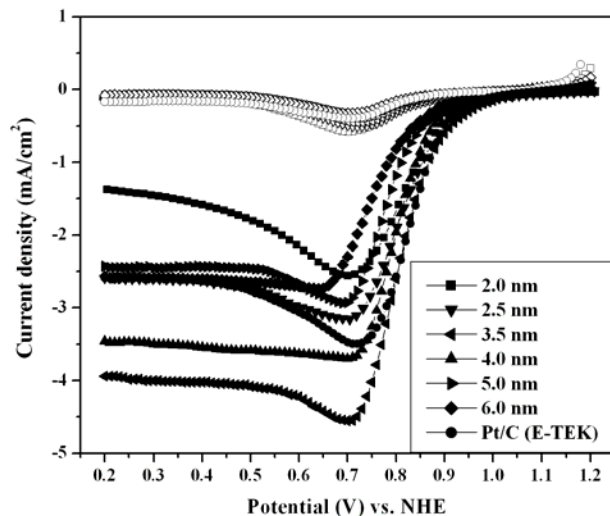
Fig. 1. Linear sweep voltammograms (LSVs) of O_2 reduction on carbon supported Pt nanoparticles of different sizes in 0.5 M H_2SO_4; Scan rate – 5 mV s^{-1} (Empty and full symbols corresponding to the LSVs in Ar- and O_2- saturated 0.5 M H_2SO_4 respectively)

Table 1. Reaction conditions, size of Pt, onset potential and ORR activity of Pt/CDX975 catalysts

Reactants	Temp (˚C) and time (min)	Size of Pt on CDX975 (nm)	Onset potential for oxygen reduction (mV vs. NHE)	ORR activity at +0.7 V vs. NHE (mA cm^{-2})
Pt(acac)$_2$, 1,2-hexadecanediol, oleic acid, oleyl amine, octyl ether	290-300 30 min	2.0±0.1	+935	1.9
,,	290-300 45 min	2.5±0.2	+930	2.5
,,	290-300 60 min	3.5±0.1	+925	4.3
Pt(acac)$_2$, 1,2-hexadecanediol, nonanoic acid, nonyl amine, diphenyl ether	250-260 30 min	4.0±0.1	+915	3.4
,,	250-260 45 min	5.0±0.2	+880	2.8
,,	250-260 60 min	6.0±0.2	+865	2.2

activity was calculated by taking the difference in activity at +0.7 V vs NHE in Ar- and O_2-saturated 0.5 M H_2SO_4. The results obtained are given in Table 1. It shows that the optimum size of Pt for oxygen reduction is 3-4 nm. This is due to the alteration of energy levels associated with the particle size of Pt. The as-synthesized Pt nanoparticles of sizes, 3.5 and 4.0 nm loaded on carbon electrodes are showing comparable activity with that of commercial Pt/C (E-TEK) catalyst.

3.2. Carbon supported Pt-M (M = Fe, Co and Cr) alloy nanoparticles for oxygen reduction

Aiming to increase the catalytic activity of the ORR, various Pt alloy catalysts, such as Pt-M (where M = Fe, Co and Cr) have been investigated. Pt alloy nanoparticles were synthesized by reduction of metal precursors (platinum(II)acetylacetonate, $FeCl_2$, $Co_2(CO)_8$ and $Cr(CO)_6$) with 1,2-hexadecanediol in the presence of nonanoic acid and nonylamine as protecting agents. The purified Pt alloy nanoparticles are loaded onto carbon black (CDX975) under ultrasonic agitation to achieve 20wt.% Pt-M(1:1)/CDX975 (M = Fe, Co and Cr). The prepared materials are characterized by XRD, TEM and EDX techniques. All the catalysts exhibited the characteristic peaks of the face centered cubic (fcc) crystalline Pt. The diffraction peaks of the Pt–M/C alloy electrocatalysts were slightly shifted to higher angles with respect to the corresponding peaks of the Pt/C electrocatalyst, indicating a contraction of the lattice and alloy formation. TEM analysis shows the good dispersion of alloy nanoparticles and the presence of respective elements on carbon was confirmed by EDX. Electrode was fabricated in the same manner as described in section 3.1 and performed the electrochemical measurements by cyclic voltammetry. Cyclic voltammograms (CVs) and linear sweep voltammograms (LSVs) of as-synthesized Pt alloys in 0.5 M H_2SO_4 is shown in Fig. 2 and 3 respectively. The calculated ORR activities are given in Table 2. The results indicate that the as-synthesized 20 wt% Pt-M(1:1)/CDX975 catalysts exhibited 1.5-1.7 times higher activity compared to that of the commercial 20 wt% Pt/C (E-TEK). The higher activity of Pt alloys is due to the inhibition of formation of –OH species on Pt electrode surface, which is evident from CVs shown in fig. 2. Moreover, the overpotential on Pt alloys is 40-70 mV less compared to the commercial Pt/C catalyst.
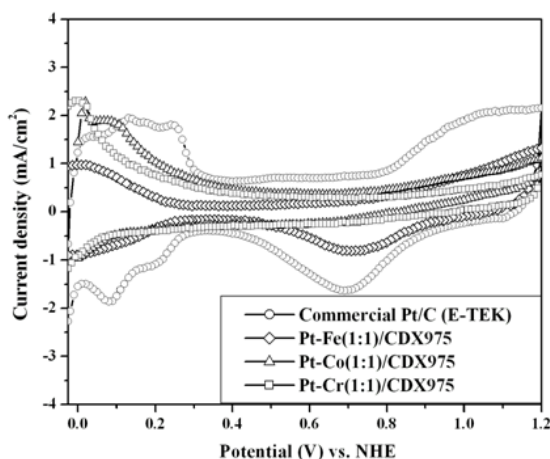
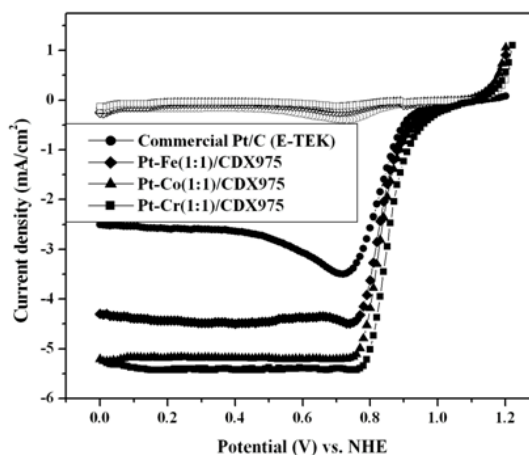Fig. 2. CVs of Pt alloys and commercial Pt/C in Ar-saturated 0.5 M H_2SO_4; Scan rate – 25 mV s^{-1}

Fig. 3. LSVs of ORR on Pt alloys and commercial Pt/C in 0.5 M H_2SO_4; Scan rate – 5 mV s^{-1}

Table 2. Metal loading, particle size, onset potential and ORR activities of carbon supported Pt alloys and commercial Pt/C catalysts

Catalyst	Metal loading (wt%)	Particle size (nm)	Onset potential for oxygen reduction (mV vs. NHE)	ORR activity at +0.7 V vs NHE (mA cm^{-2})
20% Pt-Cr(1:1)/CDX975	Pt – 15.3 Cr – 4.1	5.0±0.2	+990	5.2
20% Pt-Co(1:1)/CDX975	Pt – 15.1 Co – 4.5	5.0±0.2	+975	5.0
20% Pt-Fe(1:1)/CDX975	Pt – 15.4 Fe – 4.4	6.5±0.1	+955	4.2
Commercial 20% Pt/C (E-TEK)	Pt – 19.8	3.7±0.4	+915	3.1

3.3. Carbon supported Pd and Pd-Co-M (M = Mo and Au) alloy catalysts for oxygen reduction

Carbon black (CDX975) supported Pd and Pd-Co-Mo alloy nanoparticles are prepared by the reduction of metal precursors with hydrazine in reverse microemulsion of water/Triton X-100/propanol-2/cyclohexane. The as-synthesized Pd-Co-M/CDX975 (M = Au and Mo) catalysts were heat-treated at 700, 800 and 900 ˚C to promote alloy formation. These materials were characterized by powder XRD, TEM and EDX techniques. X-ray

6

diffraction patterns of the as-synthesized and heat treated 20wt% Pd-Co-M(7:2:1)/CDX975 catalysts show the diffraction peaks characteristic of a face-centered cubic (fcc) Pd lattice. No appreciable change in the X-ray diffraction pattern of the as-synthesized Pd-Co-M/CDX975 was observed compared to the Pd/CDX975 which means that the metal nanoparticles were not transformed into alloy. In order to improve alloying it was heat treated at different temperatures from 700 to 900 °C. As evidenced from XRD with increasing temperature the diffraction peaks are shifted to higher angles compared to the Pd/CDX975 catalyst indicates the contraction of lattice due to alloy formation.

Oxygen reduction electrodes were fabricated in the same manner as described in section 3.1 and the electrochemical activity of the Pd, Pd alloys and commercial Pt/C (E-TEK) catalysts was determined by cyclic voltammetry. The obtained voltammograms are shown in Fig. 4 & 5. In the case of heat-treated Pd-Co-M/CDX975 (M = Mo and au) catalysts at
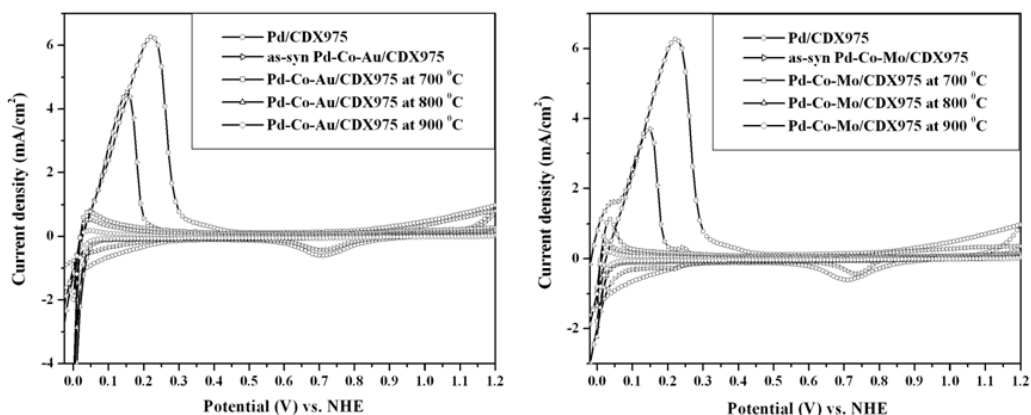

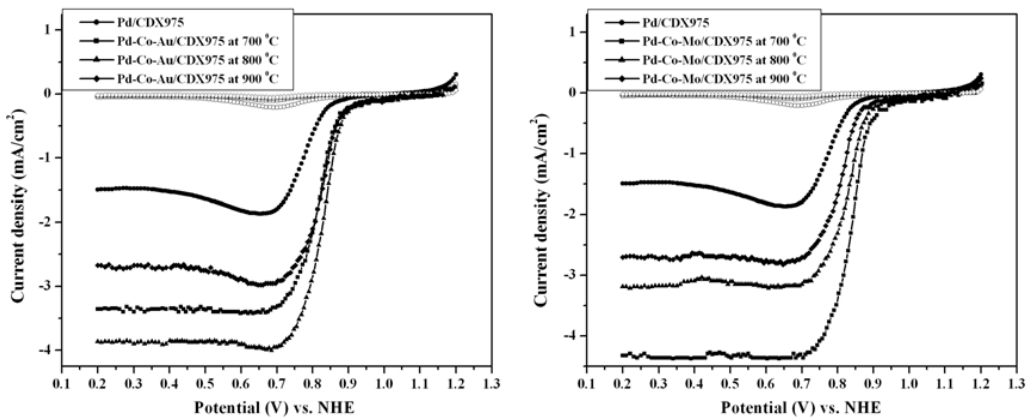Fig. 4. CVs of Pd and Pd-Co-M/CDX975 catalysts in Ar-saturated 0.5 M H_2SO_4; Scan rate: 25 mV s^{-1}

Fig. 5. LSVs of Pd and Pd-Co-M/CDX975 catalysts in Ar- and O_2- saturated 0.5 M H_2SO_4; Scan rate: 5 mV s^{-1}

Table 3. Elemental composition, crystallite size, onset potential and ORR activities of Pd, Pd alloys and commercial Pt/C catalysts

Catalyst	EDX composition Pd:Co:M (M = Mo, Au)	Crystallite size (nm)	Onset potential (mV vs. NHE)	ORR activity at +0.7 V vs NHE (mA cm^{-2})
20% Pd/CDX975	100 :- :-	1.2	+840	1.6
20% Pd-Co-Mo(7:2:1)/CDX975 at 700 ˚C	77.7:12.3:10.0	7.1	+920	4.1
20% Pd-Co-Mo(7:2:1)/CDX975 at 800 ˚C	78.3:12.6:9.1	9.4	+905	3.0
20% Pd-Co-Mo(7:2:1)/CDX975 at 900 ˚C	78.7:12.5:8.8	13.5	+865	2.6
20% Pd-Co-Au(7:2:1)/CDX975 at 700 ˚C	70.2:11.2:18.6	6.3	+875	3.3
20% Pd-Co-Au(7:2:1)/CDX975 at 800 ˚C	71.3:11.6:17.1	8.7	+905	3.9
20% Pd-Co-Au(7:2:1)/CDX975 at 900 ˚C	71.8:11.3:16.9	10.4	+880	2.9
Commercial 20% Pt/C (E-TEK)	--	3.7	+915	3.1

different temperatures, the hydrogen adsorption/desorption peaks on the surface of the Pd alloys were observed at potentials of 0.04 V vs NHE (shown in Fig. 4) showed a similar behavior to that of Pt.

The important points emerged from LSV results are, (i) Pd-Co-M/CDX975 (M = Au and Mo) catalysts exhibited the highest activity to oxygen reduction compared to the Pd/CDX975. The propensity of Pd to form PdO_x species at potentials around +0.8 V (shown in Fig. 4); the reaction inhibitor that does not take part in the reaction may be the reason of its high activity for the ORR. Among all the heat-treated Pd-Co-M/CDX975 catalysts, maximum activity was observed for the heat-treated Pd-Co-Mo/CDX975 at 700 ˚C and Pd-Co-Au/CDX975 at 800 ˚C (Table 3). Moreover, their activity is higher than that of commercial Pt/C (E-TEK) catalyst. (ii) Oxygen reduction proceeded in a relatively positive

potential region for the Pd-Co-M/CDX975 catalysts compared to the Pd/CDX975. The overpotential for ORR of the Pd alloys was ca. 50 mV less compared to that of Pd. This is due to the modification of electronic structure and alteration of energy levels of Pd by the presence of Co and Au. The differences in the onset potential for oxygen reduction at various heat-treated Pd-Co-M/CDX975 catalysts may be due to differences in the surface activation which are related to the degree of alloying, size and distribution of the metallic nanoparticles. (iii) Onset potential for oxygen reduction and shape of LSVs indicates that the ORR pathway and rate-determining step are the same on Pd-Co-M/CDX975 and Pt/C catalysts.

3.4. Carbon supported Ru_xSe_y catalysts for oxygen reduction

Carbon black (CDX975) supported Ru_xSe_y catalysts (x = 1 and y = 0-1) with a metal(s) loading of 20 wt% were prepared by the reverse microemulsion method at room temperature. The microemulsion system used in this study consisted of sodium dioctylsulfosuccinate (AOT) as a surfactant, heptane as the oil phase and either the Ru-Se precursor solution or $NaBH_4$ solution as the aqueous phase. The prepared materials were characterized by XRD, TEM and EDX. Powder XRD pattern of all the as-synthesized Ru_xSe_y/CDX975 catalysts show the peaks at 2θ values around 38°, 44°, 58°, 69°, 78° and 85° corresponding to the (100), (101), (102), (110), (103) and (112) planes of ruthenium respectively. These characteristic peaks can be assigned to *hcp* ruthenium. With the small amounts of Se to Ru in the prepared catalysts, it was found that the phase consists of *hcp* of Ru and shift of Ru diffraction lines to smaller angles indicates the solubility of Se in Ru lattice. The crystallite size of metallic nanoparticles in 20 wt% Ru_xSe_y/CDX975 catalysts estimated to be around 3.0 nm. EDX reveals the composition obtained for the as-synthesized catalysts were nearly in agreement with those of the starting metal content. Well-dispersed, uniform size and spherical shaped metallic nanoparticles with an average size of 3.1 nm on the carbon support can be seen from the TEM images. The fabricated oxygen reduction electrodes contain 70 μg_{metal} cm^{-2}. Evaluation of a series of Ru_xSe_y/CDX975 catalysts for the O_2 reduction by LSV measurements (shown in Fig. 6) reveals the improvement of ORR activity by the presence of Se with a maximum activity (geometric area-normalized current density) for the $Ru_1Se_{0.6}$/CDX975 catalyst. The reason for the improved activity is the stabilization of Ru active sites by Se against blocking as a result of (hydr)oxide formation. Moreover, the ORR

activity of as-synthesized 20 wt% $Ru_{1.0}Se_{0.6}$/CDX975 is comparable to that of the commercial 20 wt% Pt/C (E-TEK). The results obtained are given in Table 4.
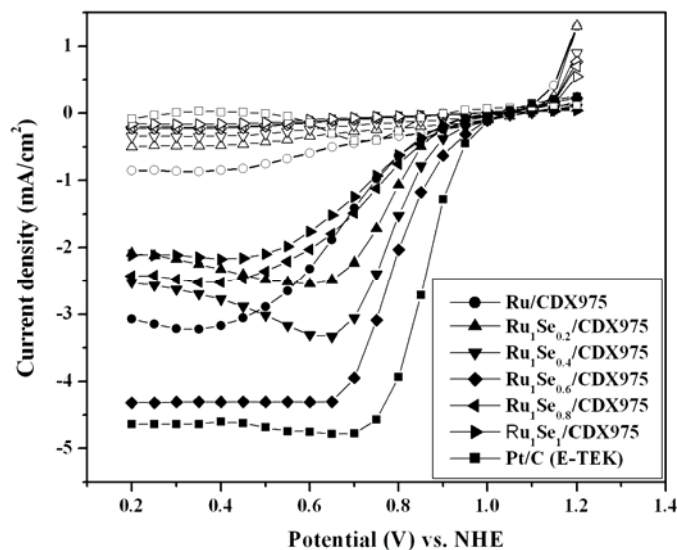

Fig. 6. Linear sweep voltammograms (LSVs) of O_2 reduction on 20 wt% Ru_xSe_y/CDX975 and commercial Pt/C (E-TEK) catalysts in 0.5 H_2SO_4; Scan rate – 5 mV s^{-1} (Empty and full symbols corresponding to the LSVs in Ar- and O_2- saturated 0.5 M H_2SO_4 respectively)

Table 4. Elemental composition, Se/Ru atomic ratio, crystallite size, onset potential for oxygen reduction and ORR activities of 20 wt% Ru_xSe_y/CDX975 (x = 1 and y = 0-1) and commercial 20 wt% Pt/C (E-TEK) catalysts

Catalyst	Elemental composition by EDX	Se/Ru atomic ratio	Crystallite size from XRD (nm)	Onset potential (mV vs. NHE)	ORR activity at +0.65 V vs. NHE (mA cm^{-2})
Ru/CDX975	100:-	0.0	3.0	+850	1.3
$Ru_1Se_{0.2}$/CDX975	87.7:12.3	0.18	3.0	+875	2.1
$Ru_1Se_{0.4}$/CDX975	76.6:23.4	0.38	3.1	+890	3.0
$Ru_1Se_{0.6}$/CDX975	68.5:31.5	0.59	3.1	+905	4.2
$Ru_1Se_{0.8}$/CDX975	62.2:37.8	0.78	3.1	+885	1.6
Ru_1Se_1/CDX975	56.2:43.8	1.00	3.1	+870	1.4
Pt/C (E-TEK)	-	-	3.7	+925	4.0

3.5. MN$_4$C$_X$ clusters (M = Fe and Co) for oxygen reduction

3.5.1. Theoretical calculations

Density functional calculations were performed to study the facile reduction of oxygen by MN$_4$ (M = Fe and Co) species. The calculated orbital energies with percentage atomic orbital contributions are given in Table 5. This study shows that the same symmetry, energy and directional nature of the HOMO of MN$_4$ (FeN$_4$: -7.20 eV and CoN$_4$: -7.72 eV) with that of the π^* orbital of O$_2$ (-8.18 eV) promotes the reduction of dioxygen in facile manner.

Table 5. Percentage atomic orbital contributions to HOMO and LUMO of MN$_4$ (M = Fe and Co) and O$_2$ by DFT method using Gaussian 98

Model System	Energy (eV)	M (Fe or Co)			N	
		s	p	d	s	p
FeN$_4$	HOMO: -7.56	0.0	0.0	30.8	0.0	69.1
	LUMO: -7.00	0.0	0.0	0.0	0.0	100.0
CoN$_4$	HOMO: -7.78	2.3	0.0	21.1	1.1	75.4
	LUMO: -7.01	0.0	1.6	3.2	1.6	93.4
		O			O	
		s		p	s	p
O$_2$	HOMO: -8.18	0.0		50.0	0.0	50.0
	LUMO: +6.41	28.3		21.7	28.3	21.7

3.5.2. Experimental

Iron tetraphenylporphyrin (FeTPP), Iron phthalocyanine (FePc) and Cobalt phthalocyanine (CoPc) complexes were synthesized, purified and adsorbed onto carbon black (CDX975). Then the resulting materials were pyrolyzed at different temperatures in Ar atm for 2 hr to produce electrocatalysts. Oxygen reduction activity of these catalysts was studied by cyclic voltammetry. The results show that the heat-treated FeTPP/CDX975 at 600 °C, FePc/CDX975 at 500 °C and CoPc/CDX975 at 600 °C displayed good activity. But the activity was less compared to the commercial Pt/C catalyst. Based on the experimental observations, metal tetramethoxyphenyl porphyrins (M-TMPP; M = Fe and Co) were synthesized, adsorbed on as-received (CDX-975, CDX1) and oxidized (HNO$_3$ treated CDX-

975, CDX2) carbon black and pyrolyzed at 800 ˚C in Ar atm for 2 hr to produce electrocatalysts for oxygen reduction. The purpose of using oxidized carbon as support is to increase the quinone groups which will increase the dispersion of metallic cluster species. The prepared Fe and Co based materials were characterized by TEM and EDX. Particle size deduced from TEM measurements (given in Table 6) indicate the good dispersion of metallic species in the case of oxidized carbon (CDX2) compared to the as-received carbon (CDX1). EDX confirms the presence of respective elements in the prepared catalysts. Oxygen reduction electrodes were fabricated to contain 56 μg_{metal} cm^{-2} and the ORR activity of the catalysts was studied by cyclic voltammetry. Higher ORR activity was observed for the heat-treated CoTMPP/CDX2 at 800 ˚C and FeTMPP-Cl/CDX2 at 800 ˚C. Moreover, the activities are comparable with that of 2 wt% Pt/Vulcan XC-72R (E-TEK). The results obtained are given in Table 6. TEM and electrochemical measurements indicate that the surface oxygen groups (quinones) introduced on the carbon support by HNO_3 treatment aid the dispersion of active species. Single cell PEMFC tests performed at 80 ˚C indicate that the performance of the heat treated M-TMPP (M = Fe and Co) supported on oxidized carbon is better compared to that of the heat treated M-TMPP (M = Fe and Co) supported on as-received carbon. At 0.7 V, CDX2-FeTMMCl(HT) and CDX2-CoTMPP(HT) catalysts yielded a current densities of ~171 and ~104 mA cm^{-2} respectively while the commercial Pt/C (E- TEK) catalyst gave a

Table 6. Estimated metal loading, particle size, ORR activity and single cell PEMFC performance of non-noble metal catalysts and commercial Pt/C catalyst

Catalyst	Metal loading (wt%)	Particle size (nm)	ORR activity at +0.7 V vs NHE (mA cm^{-2})	Single cell PEMFC performance at 0.7 V (mA cm^{-2})
CDX1-FeTMPPCl(UT)	2.01	--	0.2	--
CDX2-FeTMPPCl(UT)	2.03	--	0.35	--
CDX1-FeTMPPCl(HT)	1.96	25-37	4.2	125
CDX2-FeTMPPCl(HT)	1.97	8-15	4.9	171
CDX1-CoTMPP(UT)	1.98	--	0.16	--
CDX2-CoTMPP(UT)	1.97	--	0.24	--
CDX1-CoTMPP(HT)	1.89	35-50	3.2	82
CDX2-CoTMPP(HT)	1.93	10-18	4.5	104
Pt/Vulcan XC72R (E-TEK)	2.07	2.6	4.9	180

(UT = untreated and HT = heat-treated at 800 ˚C)

current density of ~180 mA cm^{-2}. The CDX2-FeTMPPCl(HT) and CDX2-CoTMPP(HT) catalysts show an open circuit voltage of ~0.89 and ~0.85 V respectively, which is close to that found with the commercial Pt catalyst (~0.9 V).

4. CONCLUSIONS

- Uniform size and shaped Pt nanoparticles of different sizes were prepared by polyol reduction method and loaded onto carbon black. The prepared materials were characterized by XRD, TEM and EDX. ORR measurements performed by cyclic voltammetry show that the optimum size of Pt for oxygen reduction is 3-4 nm.

- Monodispersed Pt-M alloy (M = Fe, Co and Cr) nanoparticles prepared by polyol reduction method were loaded onto carbon black and characterized by XRD, TEM and EDX. ORR measurements indicate that the Pt alloys were showing 1.5-1.7 times higher activity than commercial Pt/C (E-TEK). This is attributed to the inhibition of formation of (hydr)oxy species on Pt surface in the presence of alloying element.

- Carbon supported Pd and Pd–Co–M (M = Au and Mo) alloy catalysts were synthesized by reverse microemulsion method followed by heat-treatment and characterized by XRD, TEM and EDX. Pt like behaviour (evident from CV measurements) and comparable ORR activity of heat-treated Pd-Co-Au/CDX975 at 800 ˚C and Pd-Co-Mo/CDX975 at 700 ˚C catalysts with that of Pt/C (E-TEK) makes them as an viable oxygen reduction electrodes for electrochemical device applications.

- Reverse microemulsion method (RME) has been adopted to synthesize 20 wt% Ru$_x$Se$_y$/CDX975 catalysts. The prepared materials were characterized by XRD, SEM, TEM and EDX. ORR measurements performed at room temperature by cyclic voltammetry show that the current density exhibits a maximum for the Ru$_1$Se$_{0.6}$/C catalyst. The reason for the improved activity is the stabilization of Ru active sites by Se against blocking as a result of (hydr)oxide formation. The comparable ORR activity and stability of Ru$_1$Se$_{0.6}$/CDX975 with that of commercial Pt/C (E-TEK) catalyst makes it as an ideal cathode material for electrochemical power devices.

- DFT calculations were performed to study the electrocatalytic activity of MN$_4$ (M = Fe and Co) for the reduction of O$_2$. This study shows that the same symmetry, energy

13

and directional nature of the HOMO of FeN$_4$ with that of the π^* orbital of O$_2$ initiates and facilitates its reduction.

- The role exerted by the oxygenated surface groups in the dispersion of active species responsible for oxygen reduction was studied. The results show that the introduction of surface oxygen complexes (quinones) on carbon support increases the catalytic activity and favours the facile reduction of oxygen to water. As per the half-cell measurements, stability and single cell performance tests, MN$_4$C$_x$ (M = Fe and Co) species are the potential candidates to replace Pt for oxygen reduction.

5. REFERENCES

1. **Colmenares, L., Z. Jusys, R.J. Behm** (2007) Activity, Selectivity, and Methanol Tolerance of Se-Modified Ru/C Cathode Catalysts, *J. Phys. Chem. C* **111**, 1273-1283.

2. **Ferna´ndez, J.L., D.A. Walsh, A.J. Bard** (2005) Thermodynamic Guidelines for the Design of Bimetallic Catalysts for Oxygen Electroreduction and Rapid Screening by Scanning Electrochemical Microscopy. M-Co (M: Pd, Ag, Au), *J. Am. Chem. Soc.* **127**, 357-365.

3. **Gasteiger, H.A., K. Shyam, S. Bhaskar, F.T. Wagner** (2005) Activity benchmarks and requirements for Pt, Pt-alloy, and non-Pt oxygen reduction catalysts for PEMFCs *Appl. Catal. B: Environmental* **56**, 9-35.

4. **Kinoshita, K** (1990) Particle size effects for oxygen reduction on highly dispersed platinum in acid electrolytes, *J. Electrochem. Soc.* **137**, 845-848.

5. **Lefe´vre, M., J. P. Dodelet, P. Bertrand** (2005) Molecular Oxygen Reduction in PEM Fuel Cell Conditions: ToF-SIMS Analysis of Co-Based Electrocatalysts, *J. Phys. Chem. B* **109**, 16718-16724.

6. **Mukerjee, S., S. Srinivasan, M.P. Soriaga, J. McBreen** (1995) Effect of Preparation Conditions of Pt Alloys on Their Electronic, Structural, and Electrocatalytic Activities for Oxygen Reduction-XRD, XAS, and Electrochemical Studies, *J. Phys. Chem.* **99**, 4577-4589.

7. **Raghuveer, V., A. Manthiram, A. J. Bard** (2005) Pd-Co-Mo Electrocatalyst for the Oxygen Reduction Reaction in Proton Exchange Membrane Fuel Cells, *J. Phys. Chem. B* 109, 22909-22912.

8. **Ralph, T.R., M.P. Hogarth** (2002) Catalysis for low temperature fuel cells part 1: the cathode challenges, *Platinum Met. Rev.* **46**, 3-14.

9. **Schulenburg, H., S. Stankov, V. Schunemann, J. Radnik, I. Dorbandt, S. Fiechter, P. Bogdanoff, H. Tributsch** (2003) Catalysts for the Oxygen Reduction from Heat-Treated Iron(III) Tetramethoxyphenylporphyrin Chloride: Structure and Stability of Active Sites, *J. Phys. Chem. B* **107**, 9034-9041.

10. **Tributsch, H** (2007) Multi-electron transfer catalysis for energy conversion based on abundant transition metals, *Electrochim. Acta* **52**, 2302–2316.

6. PROPOSED CONTENTS OF THE THESIS

Chapter 1: Introduction

Chapter 2: Experimental techniques

Chapter 3: Synthesis, characterization and electrochemical studies of carbon supported Pt electrodes for oxygen reduction

Chapter 4: Synthesis, characterization and electrochemical studies of carbon supported Pt-M (M = Cr, Co and Fe) alloy electrodes for oxygen reduction

Chapter 5: Synthesis, characterization and electrochemical studies of carbon supported Pd and Pd-Co-M (M = Mo and Au) alloy electrodes for oxygen reduction

Chapter 6: Ru_xSe_y/C catalysts for oxygen reduction – A reverse microemulsion method of fabrication of electrode material

Chapter 7: MN_4C_x clusters (M = Fe and Co) – Potential oxygen reduction electrodes for PEMFC applications

Chapter 8: Summary and conclusions

7. LIST OF PUBLICATIONS BASED ON THE RESEARCH WORK

Refereed Journals

1. **Ch. Venkateswara Rao and B. Viswanathan** (2004) Oxygen reduction by FeN_4 – A DFT study, *Indian J. Chem.* A 43A (11), 2333-2335.

2. **B. Viswanathan, Ch. Venkateswara Rao and U.V. Varadaraju** (2006) On the search for non-noble metal based electrodes for oxygen reduction reaction, *Photo/Electrochemistry & Photobiology in the Environment, Energy and Fuel* 43-101.

3. **Ch. Venkateswara Rao and B. Viswanathan** (2007) Ru_xSe_y/C electrodes for oxygen reduction – A reverse microemulsion method of fabrication of electrode material, *J. Phy. Chem. C* 111, 16538-16543.

Presentations in Conferences

1. **Ch. Venkateswara Rao and B. Viswanathan** (2004) **'**Oxygen reduction by $FeN_4^{'}$ – as seen by Density Functional Approach, *National workshop on the Advances in Catalysis*, January 6 - 7th 2004, Loyola college, Chennai, India.

2. **Ch. Venkateswara Rao, B. Viswanathan and U.V. Varadaraju** (2006) Nanoparticle Pt loaded carbon materials as cathodes for possible fuel cell applications, *Indo-Australian Symposium on Nanoscience and Nanotechnology*, March 31st - April 1st 2006, Indian Institute of Science, Bangalore, India.

3. **Ch. Venkateswara Rao, B. Viswanathan and U.V. Varadaraju** (2006) The ORR activity of polyol reduced platinum on carbon electrodes – Role of crystal planes on activity, *Taiwan-India Conference on Nanomaterials,* Dec 11-12th 2006, Lunghwa University of Science and Technology, Taouyen, Taiwan. (Received best poster award)

4. **B. Viswanathan and Ch. Venkateswara Rao** (2006) Metallic nanomaterials decorated on carbon nanotubes as electrodes for Fuel cell applications, *Indo-Japan workshop on Nanomaterials,* Dec 4-5th 2006, Indian Institute of Chemical Technology, Hyderabad, India.

5. **Ch. Venkateswara Rao, B. Viswanathan and U.V. Varadaraju** (2007) MN_4C_x clusters – are they potential oxygen reduction electrode materials?, *18th National Symposium on Catalysis,* April 16-18th 2007, Indian Institute of Petroleum, Dehradun, India.